Journal of Civil Engineering
The Institution of Engineers, Bangladesh
Vol. CE 29, No. 1, 2001

NON-LINEAR FINITE ELEMENT ANALYSIS OF REINFORCED CONCRETE RECTANGULAR AND SKEW SLABS

Sk. Md. Nizamud-Doulah[1] and Ahsanul Kabir[2]

ABSTRACT: Non-linear finite element method using layered concept across the thickness has been adopted to study its suitability for the analysis of reinforced concrete slabs with special emphasis on skew slabs. Only material nonlinearity has been considered here. An eight-noded isoparametric Mindlin plate element based on layering technique is used to account for transverse shear deformations. The layered technique is adopted in order to allow for the progressive development of cracks through the thickness at different sampling points. The non-linear effects due to cracking and crushing of concrete and yielding of steel reinforcement are included. The material model behaviour is based on the experimental observation reported by various authors. Rectangular and specially some reinforced concrete skew slabs have been picked up as examples to demonstrate the applicability and efficiency of the method.

KEYWORDS: Material nonlinearity, reinforced concrete, skew slabs, thick plate, cracking load, smeared cracking, tension stiffening, ultimate load.

INTRODUCTION

The analysis and design of reinforced concrete skew slabs are normally based on the linear elastic theories and limited up to yield load only. Desayi and Prabhakara (1981) proposed a method of predicting the load deflection behaviour beyond the yield load considering the effect of membrane forces. Elastic and yield load theories can not be used in case of complex structures with complicated loading and boundary conditions. For many structures, cracking and crushing in the concrete through the depth as well as yielding of reinforcing steel are major sources of material nonlinearity. Cracking results in the permanent loss of both tensile stiffness and tensile strength in a direction normal to the crack. In case of crushing, the concrete is simply assumed to lose its entire rigidity and strength in all directions. There is little information in the literature on the behaviour of reinforced concrete skew slabs loaded to failure, whereas most of the research has been done in respect to rectangular slabs. Non-linear finite element analyses of this type of slabs have been carried out by Johnarry (1979), Cope and Rao (1981), El-Hafez (1986) and Kankam and Dagher

1 Department of Civil Engineering, BIT, Rajshahi, Bangladesh.

2 Department of Civil Engineering, BUET, Dhaka 1000, Bangladesh

(1995). More research is needed to establish the effective numerical procedure for the non-linear analysis of reinforced concrete skew slabs. This work is an attempt towards that end to correlate the experimental behaviour of few skew and rectangular slabs with the numerical predictions using simple and popularly accepted material models.

The application of the finite element method to the analysis of concrete structures has been growing rapidly since Ngo and Scordelis (1967) first introduced it. The success of analysis depends on an appropriate modelling of the composite material behaviour. Many material models (Chen and Ting (1980), Gupta and Akbar (1984), Hu and Schnobrich (1990), Gopalakrishnan, Mohan Rao, and Appa Rao (1993)) have been proposed to predict the response of concrete. However, they include a large number of functions and material parameters and involve tedious programming and computational effort. An ideal choice is one that is simple and involves as few parameters as possible, yet can yield reasonably accurate results. From this point of view, the model proposed by Kupfer et al. (1969) with a slight modification is incorporated here. This model is simple and is found to work well with Mindlin (1965)-plate formulation. This study present numerical model based on layered Mindlin plate element formulations. The load deflection behaviour of reinforced concrete skew slabs in particular and some rectangular slabs have been studied. The ultimate load carrying capacities determined numerically are compared with the available experimental data and/or other theoretical solutions.

MINDLIN PLATE FORMULATION

An eight-noded isoparametric element using layered representation is incorporated in this study. The displacement u, v, w at any point can be expressed as:

$$\begin{bmatrix} u(x,y,z) \\ v(x,y,z) \\ w(x,y,z) \end{bmatrix} = \begin{bmatrix} u_0(x,y) - z\theta_x(x,y) \\ v_0(x,y) - z\theta_y(x,y) \\ w_0(x,y) \end{bmatrix} \quad (1)$$

Where uo, vo, wo are the displacements at the plate mid-surface, θ_x and θ_y are the rotations of the normal along x and y-axes. The displacements are interpolated as follows:

$$\underline{U} = \Sigma \underline{N}_i \underline{d}_i \quad (2)$$

where $\underline{U} = \{u, v, w\}^T$

$$\underline{N}_i = N_i \begin{bmatrix} 1 & 0 & 0 & -z & 0 \\ 0 & 1 & 0 & 0 & -z \\ 0 & 0 & 1 & 0 & 0 \end{bmatrix}$$

N_i = shape function for node i expressed in terms of natural coordinates (ξ,η)

$$\underline{d}_i = \{u_i, v_i, w_i, \theta_{xi}, \theta_{yi}\}^T$$

In the two dimensional analysis based on plane stress assumption, the strain is related to displacement as:

$$\underline{\varepsilon}_p = \Sigma \underline{B}_{pi} \underline{d}_i$$

$$\underline{\varepsilon}_s = \Sigma \underline{B}_{si} \underline{d}_i \qquad (3)$$

where $\underline{\varepsilon}_p = \{\varepsilon_x, \varepsilon_y, \gamma_{xy}\}^T$,

$$\underline{\varepsilon}_s = \{\gamma_{xy}, \gamma_{zx}\}^T$$

Bpi = strain matrix due to plane stress deformation
$\underline{\mathbf{B}}_{si}$ = strain matrix due to transverse shear deformation

The following are the incremental stress-strain relationships

$$\underline{\Delta\sigma}_p = \underline{D}_p \underline{\Delta\varepsilon}_p$$

$$\underline{\Delta\sigma}_s = \underline{D}_s \underline{\Delta\varepsilon}_s \qquad (4)$$

$$\underline{\Delta\sigma}_s^T = (\Delta\tau_{xz}, \Delta\tau_{yz})$$

$$\underline{\Delta\varepsilon}_s^T = (\Delta\gamma_{xz}, \Delta\gamma_{yz})$$

$\underline{\mathbf{D}}_p$ = elasticity matrix related to in-plane stresses
$\underline{\mathbf{D}}_s$ = elasticity matrix related to transverse shear stresses

The stiffness matrix and the load vectors are obtained from the following expressions

$$\underline{K}_{ij} = \int_V \underline{B}_{pi}^T \underline{D}_p \underline{B}_{pj} dV + \int_V \underline{B}_{si}^T \underline{D}_s \underline{B}_{sj} dV$$

$$\underline{f}_i = \int_V \underline{N}_i^T \underline{b} dV + \int_s \underline{N}_i^T \underline{t} ds \qquad (5)$$

where, $\underline{\mathbf{b}}$ = body forces
$\underline{\mathbf{t}}$ = boundary tractions

MATERIAL MODELLING

Modelling of Concrete Behaviour

The uniaxial stress-strain curve for concrete is idealised as shown in Fig. 1. The concrete is considered as an isotropic bilinear elastic material in compression. The experimentally determined failure envelope of Kupfer et al (1969) under biaxial stress condition is shown in Fig. 2. The mathematical description of this surface given by Kupfer and Gerstle (1973) in the biaxial principal stress space has been included in this study without any modification for compressive state of stress. Thus the failure surface under biaxial compression is given by:

$$F(\sigma)=\left(\frac{\sigma_1}{f'_c}+\frac{\sigma_2}{f'_c}\right)^2-\frac{\sigma_2}{f'_c}-3.65\,\frac{\sigma_1}{f'_c}=0 \qquad (6)$$

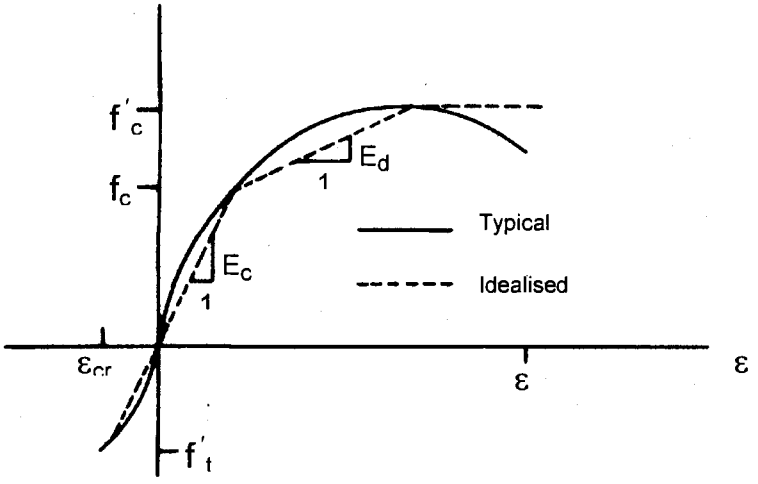

Fig 1. Typical and Idealised Uniaxial Behaviour of Concrete

The initial discontinuous surface under biaxial compression stress state is obtained by approximately scaling down the assumed failure surface to correspond the uniaxial bilinear stress-strain curve. Local failure of local sampling point occurs when the following crushing criterion is fulfilled.

$$F(\varepsilon)=\sqrt{\varepsilon_x^{\,2}+\varepsilon_y^{\,2}-\varepsilon_x\varepsilon_y+0.75\gamma_{xy}^{\,2}}=0 \qquad (7)$$

When the failure surface in biaxial compression is reached the constitutive relation is made zero. If the crushing criterion as given by

Eq. (7) is satisfied the material is assumed to lose its entire strength and rigidity in all directions and the current stresses are set to zero.

The failure envelope of Kupfer et al (1969) has been selected for biaxial tension-tension and tension-compression state of stresses with a little modification. When concrete is subjected to a combined tension-compression stress state, the failure surface is defined as:

$$F(\sigma)=\frac{\sigma_1}{f_t'}-\frac{\sigma_2}{f_c'}-1=0 \qquad (8)$$

The failure surface for biaxial tension-tension stress state is defined as

$$F(\sigma) = \sigma_1 - f_t' = 0 \qquad (9)$$

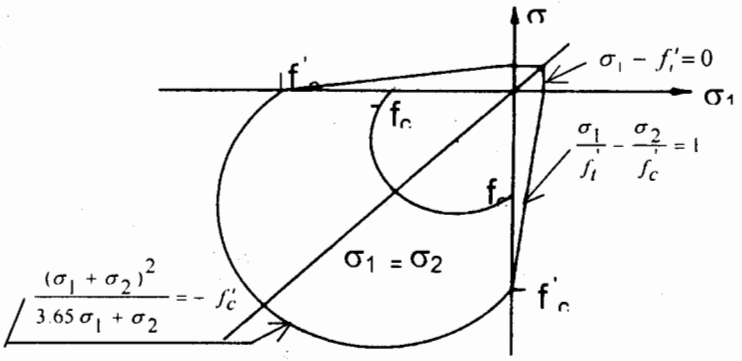

Fig 2. Idealised Biaxial Strength Envelope for Concrete

When the stresses in a layer equal or exceed the failure envelopes of Eq. (8) and Eq. (9) concrete is assumed to crack normal to the offending principal stress. Cracking of concrete is represented by many finely spread smeared cracks and thus cracking is incorporated into the stiffness properties of the concrete as an orthotropic material. A smeared crack model allows the concrete to crack in one or two directions and for the cracks to partially or fully close. The local discontinuities due to cracking are represented in a distributed manner by this approach. This is a major advantage of this model. The angle between the crack and the positive x-axis is measured counter-clockwise positive as shown in Fig. 3 and may be deduced from:

$$\tan 2\theta=\frac{\tau_{xy}}{(\sigma_x-\sigma_y)/2} \qquad (10)$$

After formation of the first crack, the concrete is assumed to lose its stiffness perpendicular to the crack direction. The crack oriented local elasticity matrix is transformed to global co-ordinate system standard strain transformation matrix T_ε as:

$$\underline{C}_G = \underline{T}_\varepsilon^T \underline{C}_L \underline{T}_\varepsilon \quad (11)$$

where, C_L = local elasticity matrix

C_G = global elasticity matrix

$$T_\varepsilon = \begin{bmatrix} c^2 & s^2 & cs \\ s^2 & c^2 & -cs \\ -2cs & 2cs & (c^2 - s^2) \end{bmatrix}$$

where, c = cos θ_{cr}, s = sin θ_{cr}, and θ_{cr} = angle with respect to x-axis.

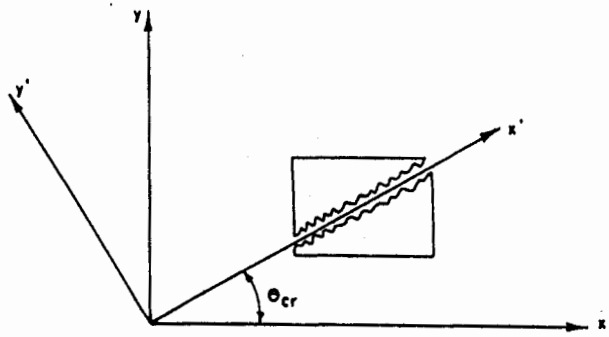

Fig 3. Crack Orientation w.r.t. x-axis

Concrete cracked in two directions is assumed to lose all of its strength. The tension stiffening effect of concrete is included by allowing concrete stress normal to the crack to gradually drop to zero over a specified strain range as shown in Fig. 4. The tension stiffening approach with n=15 suggested by Clark and Speirs (1978) ensures good predictions for slabs and beams. The value assigned to 'n' was 10 and 20 in this analysis.

Modelling of Reinforcing Steel Behaviour

Reinforcing steal is assumed to be smeared into a thin layer of thickness equivalent to its total area. The smeared layer of steal is assumed to have unidirectional stiffness corresponding to the direction of its physical layout as shown in Fig. 5. This model describes a nonlinear stress-strain relationship proposed by Richard and Abbott (1975). The experimental stress-strain curve of reinforcing steel loaded monotonically is shown in Fig. 6. A procedure is developed to fit a smooth analytical expression to this experimentally obtained stress-strain curve. The proposed equation is given by

$$\sigma = \frac{E_1\varepsilon}{\left(1+\left|\frac{E_1\varepsilon}{\sigma_0}\right|^n\right)^{\frac{1}{n}}} + E_p\varepsilon \qquad (12)$$

In which referring to Fig. 6, $E_1 = E_s - E_P$, E_s = initial modulus of elasticity of steel, E_P = plastic modulus chosen as the slope at a convenient point at the ultimate zone, n = shape parameter of the stress-strain curve, and σ_0 = a reference plastic stress.

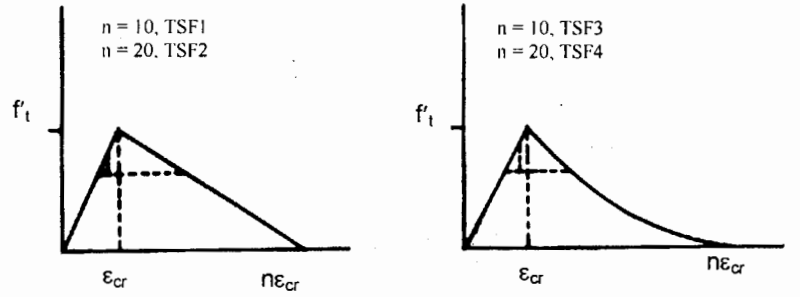

(a) Linear decay (b) Parabolic decay

Fig 4. Typical Tension Stiffening Curves for Concrete

The shape parameter n may be obtained by forcing the analytical expression Eq.12 passing through two points (ε_a, σ_a; ε_b, σ_b) on the stress-strain curve as shown in Fig. 6, where, for convenience $\varepsilon_b = 2\varepsilon_a$. The resulting equation is

$$A^n - 1 = \frac{1}{2^n}(B^n - 1) \qquad (13)$$

In which, $A = E_1/(E_a - E_P)$, $B = E_1/(E_b - E_P)$, $E_a = \sigma_a/\varepsilon_a$ and $E_b = \sigma_b/\varepsilon_b$.

The shape parameter n is then obtained by numerical iteration of Eq.13. The parameter σ_0 is obtained using trial values of n

$$\sigma_0 = \frac{E_1\varepsilon}{\left(A^n - 1\right)^{\frac{1}{n}}} \qquad (14)$$

The expression for the tangent modulus is obtained by differentiating Eq.12 with respect to strain as

$$E_t = \frac{E_1}{\left(1+\left|\frac{E_1\varepsilon}{\sigma_o}\right|^n\right)^{\frac{n+1}{n}}} + E_p \qquad (15)$$

The steel is oriented at an angle ϕ_s measured counterclockwise from the x-axis. The local modulus matrix is transformed to the global axis with the help of transformation matrix.

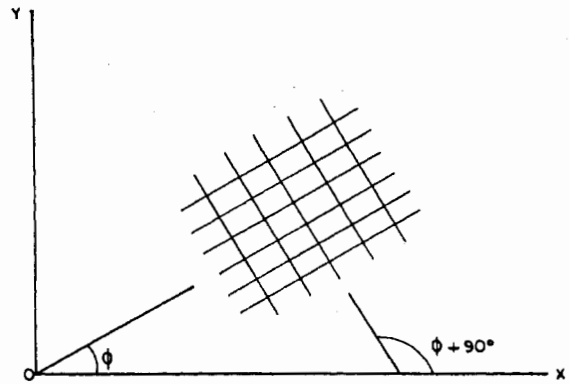

Fig 5. Typical Layout of Reinforcing Steel

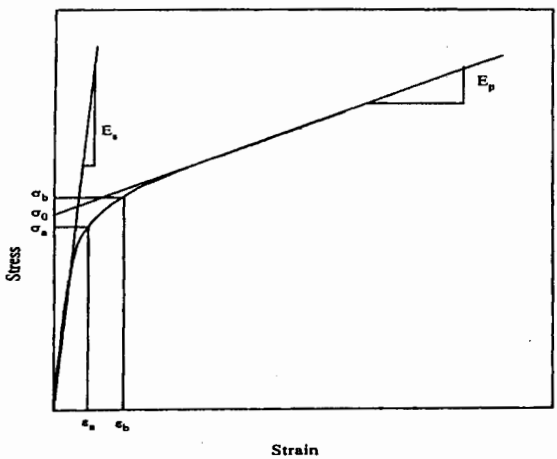

Fig 6. Modeling Stress-Strain Relationship of Reinforcing Steel

RESULTS AND DISCUSSION

Finite element discretisation eventually results in a set of simultaneous equations of the form

$$\underline{\mathbf{K}}\,\underline{\mathbf{d}} = \underline{\mathbf{R}} \qquad (16)$$

where $\underline{\mathbf{K}}$ = Element stiffness matrix
$\underline{\mathbf{d}}$ = Element displacement vector
$\underline{\mathbf{R}}$ = Element load vector

Frontal solution technique is used here where element stiffness assembly and its reduction go simultaneously. The solution of non-linear problems by the finite element method is usually attempted by one of three basic techniques - (a) Incremental methods, (b) Iterative methods and (c) Modified Newton-Raphson's method. An effective solution scheme for these equations involves the use of an incremental loading procedure with subsequent equilibrium iteration. Hence, the Modified Newton-Raphson's method in which the stiffness matrix updated at certain interval is used here in the program to improve the convergence rate. The analysis is carried out by loading the structure in small load increments. For every load increment, iterations to equilibrium are performed to the point where the residual force comes to an allowable tolerance. The stiffness is updated once in each increment at the second iteration so that the non-linear effects are reflected more accurately in the stiffness matrix. Kabir (1986) reports that this updating of stiffness matrix proves to be more efficient and economical and it is found to be so in this study. For every load step the residual load vector is calculated as the difference between the external and the internal loads:

$$\underline{\psi} = \underline{\mathbf{R}} - \int_V \underline{\mathbf{B}}^T \underline{\sigma}\, dV \qquad (17)$$

The unbalanced force is reduced to a negligibly small value iteratively by reapplying it to the structure. Displacement-norm convergence criterion with 0.1 % tolerance is used in this study to achieve convergence for the unbalanced load vector resulting from an iteration.

A small load is first applied and the maximum tensile stress developed anywhere in the concrete due to this applied load is found out. The load is then automatically scaled up to the numerical cracking load Pcr to correspond the limiting tensile strength of concrete. After cracking a load increment of λPcr is applied where λ was limited between 10 % and 20 % of the cracking load. This approach was adopted by Kabir (1986) and it is reported that this worked well with a good number of reinforced concrete slabs.

The program should be stopped as soon as some set of collapse criterion is met. Otherwise the instability conditions arising due to

decay of stiffness matrix would possibly break down the solution process long before the matrix itself becomes singular. At this stage no additional load can be sustained by the structure indicating its total failure. The displacements due to accumulation of its increment may rise sharply resulting in a lack of the convergence of the non-linear solution. The maximum admissible vertical deflection criterion indicating total collapse was used to stop the program in this study. When the deflection at any particular increment of loading exceeded a value equal to 75% of the slab thickness, the analysis was terminated and the load at that point was taken as the ultimate load.

NUMERICAL EXAMPLES

The experimental results reported by some other investigators are compared with the results obtained using this model in order to study the effectiveness and limitations of the present non-linear model. If this numerical model can produce an accurate prediction over a wide range of experimental problems for the general behaviour such as deflections, cracking loads and ultimate loads, the model can be used to predict the behaviour of any other problems. In some cases where material properties are not reported, they are assumed.

Jofriet and McNeice's Slab

The corner-supported slab reported by Jofriet and McNeice (1971) was analysed using the present non-linear model. The slab was loaded with a single concentrated load at centre span. The overall slab thickness was 1.75 inch with an effective depth of 1.31 inch. A quarter of the slab was discretised from symmetry as shown in Fig. 7. The load deflection curves are shown in Fig. 8. The respective material properties used for the analysis are :

E_c = 4150 ksi, f'_c = 5500 psi, f'_t = 550 psi, ν = 0.15
E_s = 29000 ksi, f_y = 60,000 psi, σ_0 = 50,000 psi, n = 2.67
$\rho_x = \rho_y$ = 0.85 %, t = 1.75 in, d = 1.31 in

Johnarry's Slabs (S590)

The slab tested by Johnarry (1979) designated as S590 is a rectangular slab simply supported on two opposite edges and subjected to a single concentrated load on mid span at 1/6th point from free edge. The slab dimensions are 760 mm x 1080 mm. Due to symmetry about the mid span line just one half of the slab is taken for analysis and discretised with 12 elements as shown in Fig. 9. The load-deflection behaviour for this slab is shown in Fig. 10. The material properties for both the slabs are :

E_c = 14700 N/mm^2, f_{cu} = 21 N/mm^2, f'_t = 2.1 N/mm^2
E_s = 200000 N/mm^2, f_y = 250 N/mm^2, σ_0 = 230 N/mm^2, n = 2.67
t = 38 mm, d = 32 mm, ν = 0.2

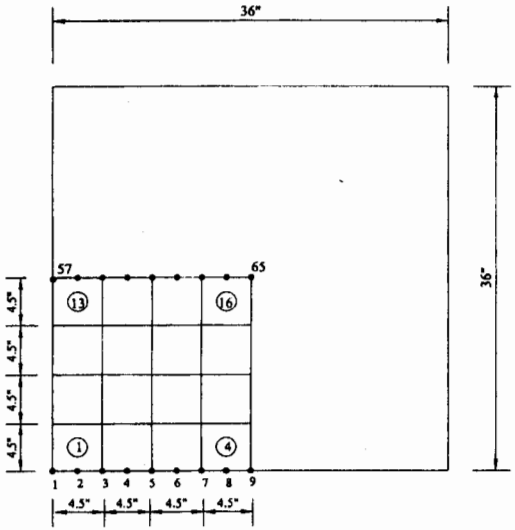

Fig 7. Element Discretisation for McNeice's Slab

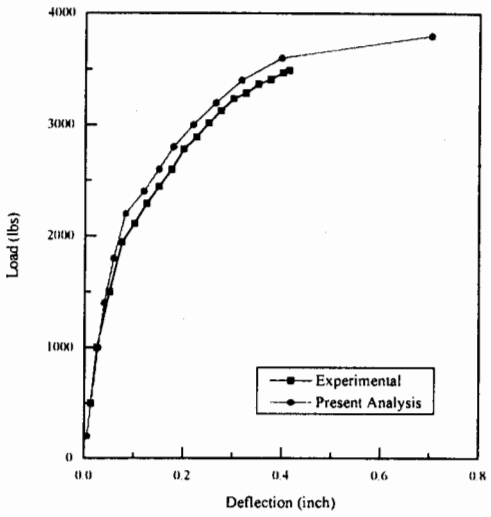

Fig 8. Load vs. Displacement Curve for Central Node of McNeice's Slab

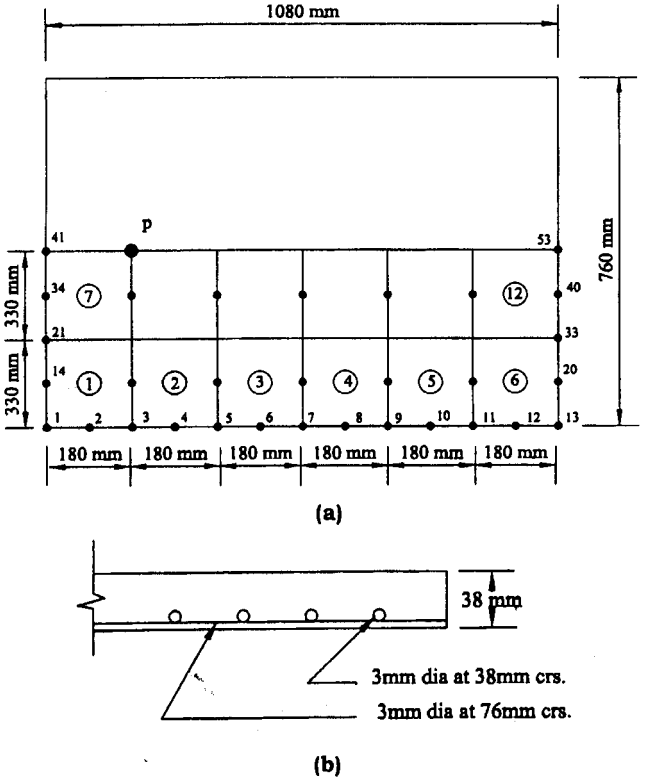

Fig 9. Element Grid for Johnarry's Slab S590

El-Hafez's Skew Slab (Model No. 2)

One of the skew slabs designated as Model No. 2 with 60° skew angle supported on two opposite edges and tested by El-Hafez (1986) are selected for analysis. Fig. 11 shows the dimensions, element grid system adopted and loading arrangement for the slab. 6, 8, 10 and 12 mm diameter high yield deformed bars were used in the model for different layers and orientations. For bottom longitudinal direction parallel to the free edge, chiefly 12-mm dia. bars were used except for elements 1, 2, 6, 7, 24, 25, 29 and 30. These later elements were reinforced mostly with 8-mm dia. bars. For bottom transverse direction parallel to the support edge, mainly 10-mm dia. bars were used. The equivalent steel layer thickness for both directions were considered for computer implementation. Fig. 12 shows the curves to represent the load-deflection behaviour for the slab. The material properties for concrete and steel are as follows:

E_c = 29250 N/mm², $f'c$=36 N/mm², $f't$= 3.4 N/mm², ν = 0.2
E_s = 211600 N/mm², fy= 500 N/mm ², σ_0 = 500 N/mm², n = 2.67
t = 100 mm, d = 85 mm

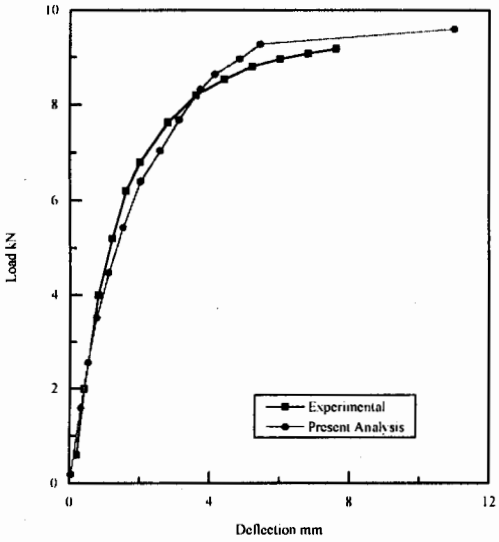

Fig 10. Load vs. Displacement Curve for Johnarry's Slab S590

The experimental results for the examples described above are compared with the numerical results obtained in the present study in table 1.

Table 1. Comparison of Experimental Loads with the Present Numerical Investigation

Slab Designation	Cracking Load		Ultimate Load	
	Experimental	Present Analysis	Experimental	Present Analysis
McNiece's Slab (lbs)	___	1000	3490	3800
Johnarry's Slab (kN)	___	1.6	9.18	9.60
El-Hafez's Slab (kN)	42.0	32.7	176.5	181.4

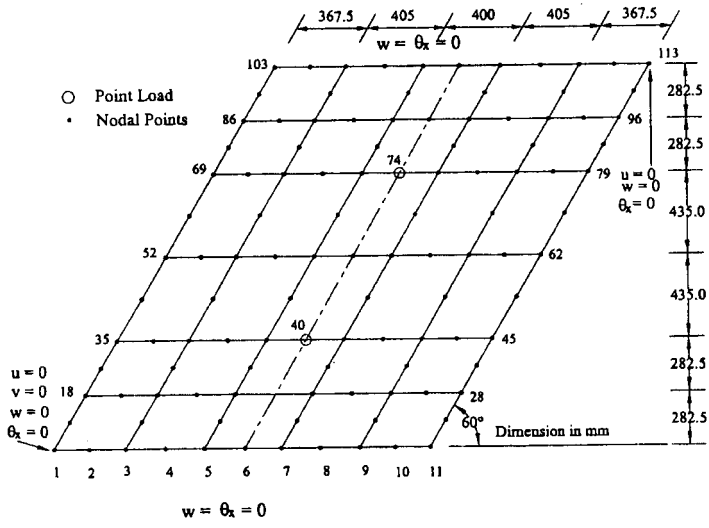

Fig 11. Element Mesh with Boundary Conditions and Loading for El-Hafez's Slab Model No. 2

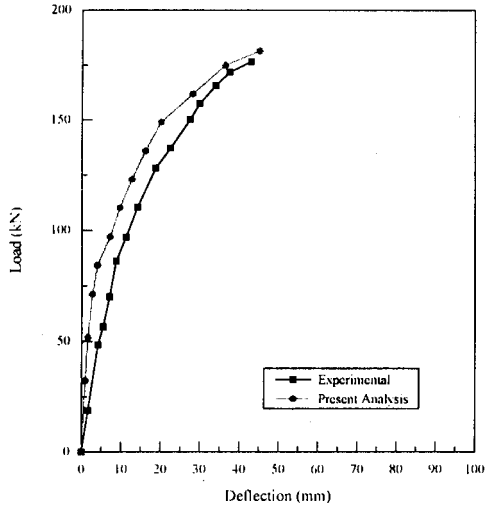

Fig 12. Load vs. Displacement Curve for Node No. 40 for El-Hafez's Slab Model No. 2

CONCLUSIONS

Comparison of the numerical predictions with the experimental results demonstrates that the layering technique may suitably be employed for analysing reinforced concrete slabs including skew ones. The good agreement obtained in these examples between the numerical and the experimental results indicates that the present proposed computational model may be efficiently used with good accuracy. The material model is perfectly general and so may be used for any arbitrarily shaped reinforced concrete plates. It is useful in predicting the cracking and ultimate load carrying capacity of reinforced concrete slabs. Comparing the numerical load-deflection curves with the experimental, it may be concluded that the model is able to predict the entire sequence fairly well under monotonically increasing transverse load for reinforced concrete skew slabs. The material models adopted for layered concrete and steel reinforcement are simple and may be adopted for numerical analysis of reinforced concrete skew slabs.

REFERENCES

Chen, W.F. and Ting, E.C. (1980), "Constitutive Models for Concrete Structures", Jnl. Engrg. Mech. Div., ASCE, Vol. 106, No. 1, pp. 1-19.

Clark, L.A. and Speirs, D.M. (1978), "Tension Stiffening in Reinforced Concrete Beams and Slabs under Short Term Loads", Technical Report, 42.521, Cement and Concrete Association.

Cope, R. J. and Rao, P. V. (1981), "Non-linear Response of Reinforced Concrete Skewed Slab Bridges", University of Liverpool, 1 Research Report.

Desayi, P. and Prabhakara, A. (1981), "Load-Deflection Behaviour of Restrained Reinforced Concrete Skew Slabs", Jnl. of Struct. Div., ASCE, Vol. 107, No. ST5, pp. 873-888.

El-Hafez, L.M.A. (1986), "Direct Design of Reinforced Concrete Skew Slabs", Ph.D. Thesis, Dept. of Civil Engrg., University of Glasgow.

Gopalakrishnan, S., Mohan Rao, S.V.K. and Appa Rao, T.V.S.R. (1993), "Non-linear Analysis of Reinforced Concrete Hyperboloid Cooling Towers-1 - Material Model, Finite Element Model and Validation, Computers and Structures", Vol. 49, No. 6, pp. 913-921.

Gupta, A. K. and Akbar, H. (1984), "Cracking in Reinforced Concrete Analysis", Jnl .Struct. Engrg. Div., ASCE, Vol. 110, No. 8, pp. 1735-1746

Hu, H. T. and Schonobrich, W. C. (1990), "Non-linear Analysis of Cracked Reinforced Concrete", Jnl. of ACI (Struct), Vol. 87, No. 2, pp. 199-207.

Jofriet, J.C. and McNeice, G.M. (1971), "Finite Element Analysis of Reinforced Concrete Slabs", Jnl. Struct. Div., ASCE, Vol. 97, No. ST5, pp. 785-806.

Johnarry, T. (1979), "Elastic-Plastic Analysis of Concrete Structures", Ph.D. Thesis, University of Strathclyde.

Kabir, A. (1986), "Non-linear Analysis of Reinforced Concrete Structural Slabs", Ph.D. Thesis, University of Strathclyde.

Kankam, J. A. and Dagher, H. J. (1995), "Non-linear FE Analysis of RC Skewed Slab Bridges", Jnl. Struct. Engrg. Div., ASCE, Vol. 121, No. 9, pp. 1338-1345.

Kupfer, H., Hilsdorf H.K. and Rusch, H. (1969) "Behaviour of Concrete under Biaxial Stresses", Jnl. of ACI, Vol. 66, No. 8, pp. 656-666.

Kupfer, H.B. and Gerstle, K.H. (1973), "Behaviour of Concrete under Biaxial Stresses", Jnl. of Engg. Mech. Div., ASCE, Vol. 99, No. EM4, pp. 853-866.

Mindlin, R. D. (1965), "Influence of Rotatory Inertia and Shear on Flexural Motion of Isotropic Elastic Plates", Jnl. of Appl. Mech., Vol. 18, pp. 31-38.

Ngo, D. and Scordelis, A. C. (1967), "Finite Element Analysis of Reinforced Concrete Beams", Jnl. of ACI, Vol. 64, No. 3, pp. 152-163.

Richard, R.M. and Abbott, B.J. (1974), "Versatile Elastic-Plastic Stress-Strain Formula", J. Eng. Mech. Div, ASCE, Vol. 101, No. EM4, pp. 511-515.